

Lattice dynamics of GaSb

Marvin K. Farr,* Joseph G. Traylor, and S. K. Sinha

Ames Laboratory—USAEC and Department of Physics, Iowa State University, Ames, Iowa 50010

(Received 8 July 1974)

The lattice dynamics of gallium antimonide has been investigated experimentally using the method of coherent inelastic scattering of thermal neutrons. The frequencies for phonons propagating in the [001], [111], and [110] symmetry directions in an undoped gallium antimonide crystal at 300 K have been determined with an estimated precision of 2%. The sample had a carrier concentration of 4.85×10^{17} holes/cm³ (upper limit) at 300 K. Both second-neighbor and first-neighbor shell models (SM) were fitted to the measured phonon dispersion curves. Some systematic trends among the fitted parameters for the first-neighbor SM for the gallium group-V compounds (GaP, GaAs, and GaSb) are discussed. The fitted second-neighbor SM parameters have been used to generate a phonon frequency distribution, which in turn has been used in the calculation of the temperature dependence of the specific heat at constant volume and the Debye Θ .

I. INTRODUCTION AND EXPERIMENT

Gallium antimonide is one of several group III-V compounds which have been widely studied because of their important semiconducting properties. The lattice vibrations play an important role in determining the dielectric and infrared optical properties of these crystals as well as their free-carrier transport properties. Hence it is of considerable interest to study the phonon dispersion curves of GaSb and to compare the results with those of the other $A^{III}B^V$ semiconductors whose phonon spectra have been measured. Such measurements have been published for GaAs,¹ GaP,² and InSb.³ We present here the results of an experimental investigation, a shell-model calculation of the lattice dynamics of GaSb, and a comparison of these results with the results for GaAs, GaP, and InSb. In particular, we now have a good basis for comparing the three gallium compounds.

The experimental measurements were conducted at room temperature on a single crystal (volume approximately 11 cm³) of undoped GaSb. A Hall-effect measurement of the upper limit of the carrier concentration in the sample showed 4.85×10^{17} holes/cm³ at 300 K.

The phonon dispersion curves were measured on a triple-axis spectrometer at the Ames Laboratory Research Reactor (ALRR). The constant- Q technique was used throughout the experiment under conditions of fixed incident neutron energy E_0 . To improve the resolution and still allow the necessary momentum transfer, we utilized three different values of E_0 : 21, 30, and 55 meV. Most of the measurements were made using neutron energy-loss processes, although a few measurements were taken with energy gain. The sample had a mosaic spread of less than 6' of arc; thus, it was necessary to use care in alignment to account for extinction effects.

Before beginning the measurements we calculated

the inelastic coherent neutron structure factors for accessible points in reciprocal space, using the InSb shell-model (SM) parameters of Ref. 3. Following the measurement of several acoustical phonons, we calculated a preliminary set of SM parameters for GaSb and then used these for subsequent structure-factor calculations. We employed both structure-factor information and neutron-focusing techniques whenever possible in the experiment.

II. RESULTS

The following branches of the phonon dispersion curves of GaSb were measured (T, L, A, and O indicate the transverse, longitudinal, acoustic or optic modes, respectively, I and II indicate mixed modes, and the irreducible representation² of each mode is given in parentheses): TA (Δ_3), LA (Δ_1), TO (Δ_3), LO (Δ_1) along the [001] direction; TA (Λ_3), LA (Λ_1), TO (Λ_3), LO (Λ_1) along the [111] direction; TA (Σ_2), IA (Σ_1), IIA (Σ_1), TO (Σ_2), IO (Σ_1), IIO (Σ_1) along the [110] direction.

A nonlinear least-squares-fitting program was used to fit a Gaussian function to each of the measured phonon peaks. The program allowed fitting of two Gaussian functions, a Lorentzian function, and a cubic polynomial background function to a measured neutron group. However, in most cases a good fit was obtained using only one or two Gaussian functions and a linear background. The phonon frequencies listed in Table 1 are the centers of the fitted Gaussian functions. When a particular phonon was measured more than once, the frequency shown is a suitably weighted average of the fitted centers.

We have estimated our experimental errors according to the following: (i) instrumental error (systematic), (ii) statistical error in the neutron counting process (random), and (iii) sample alignment errors (systematic for a particular set of

TABLE I. Phonon frequencies in GaSb at 300 K. $\zeta = a_0q/2\pi$, $a_0 = 6.0959 \text{ \AA}$.^a

ζ	$\Delta_3(\text{A})$	$\Delta_1(\text{A})^{[1001]}$	$\Delta_3(\text{O})$	$\Delta_1(\text{O})$		
0.0			6.87 ± 0.14			
0.1			6.83 ± 0.14	7.0 ± 0.2		
0.2	0.839 ± 0.017	1.289 ± 0.026	6.69 ± 0.13	7.05 ± 0.14		
0.3	1.174 ± 0.023	1.900 ± 0.038				
0.4	1.444 ± 0.029	2.466 ± 0.049	6.41 ± 0.13	6.95 ± 0.14		
0.5	1.593 ± 0.032	3.034 ± 0.060				
0.6	1.689 ± 0.034	3.542 ± 0.071	6.37 ± 0.13	6.73 ± 0.14		
0.7	1.702 ± 0.034	4.01 ± 0.08				
0.8	1.716 ± 0.034	4.45 ± 0.09	6.33 ± 0.13	6.45 ± 0.13		
0.9	1.712 ± 0.034	4.80 ± 0.10				
1.0	1.698 ± 0.034	4.99 ± 0.10	6.36 ± 0.13	6.35 ± 0.13		
ζ	$\Delta_3(\text{A})$	$\Lambda_1(\text{A})^{[1101]}$	$\Lambda_3(\text{O})$	$\Lambda_1(\text{O})$		
0.0			6.87 ± 0.14			
0.1	0.563 ± 0.011	1.250 ± 0.025	6.84 ± 0.14	6.9 ± 0.2		
0.15	0.851 ± 0.017	1.833 ± 0.037				
0.2	1.066 ± 0.021	2.39 ± 0.05	6.76 ± 0.14	6.81 ± 0.14		
0.25	1.206 ± 0.024	2.943 ± 0.059				
0.3	1.265 ± 0.025	3.395 ± 0.068	6.62 ± 0.13	6.56 ± 0.13		
0.35	1.333 ± 0.027	3.91 ± 0.08				
0.4	1.356 ± 0.027	4.26 ± 0.08	6.48 ± 0.13	6.33 ± 0.13		
0.45	1.353 ± 0.027	4.54 ± 0.09				
0.5	1.368 ± 0.027	4.60 ± 0.09	6.48 ± 0.13	6.15 ± 0.12		
ζ	$\Sigma_2(\text{A})$	$\Sigma_1(\text{IA})$	$\Sigma_1(\text{II A})^{[110]}$	$\Sigma_2(\text{O})$	$\Sigma_1(\text{I O})$	$\Sigma_1(\text{II O})$
0.0				6.87 ± 0.14	6.87 ± 0.14	
0.15		0.896 ± 0.018	1.419 ± 0.028			
0.2	0.929 ± 0.019	1.175 ± 0.023	1.88 ± 0.038	6.70 ± 0.13	6.74 ± 0.14	
0.3	1.269 ± 0.025	1.660 ± 0.033	2.623 ± 0.052			
0.4	1.512 ± 0.030	2.060 ± 0.041	3.18 ± 0.06	6.56 ± 0.13	6.28 ± 0.13	6.69 ± 0.13
0.5	1.681 ± 0.034	2.358 ± 0.047	3.62 ± 0.07			
0.6	1.755 ± 0.035	2.560 ± 0.051	4.07 ± 0.08	6.39 ± 0.13	5.91 ± 0.12	6.53 ± 0.13
0.7	1.779 ± 0.036	2.60 ± 0.06	4.45 ± 0.09			
0.8	1.747 ± 0.035	2.375 ± 0.047	4.60 ± 0.09	6.27 ± 0.12	5.97 ± 0.12	6.56 ± 0.13
0.9	1.710 ± 0.034	1.927 ± 0.038	4.75 ± 0.10			
1.0	1.698 ± 0.034	1.698 ± 0.034	4.99 ± 0.10	6.36 ± 0.13	6.35 ± 0.13	6.36 ± 0.13

^aReference 4.

measurements). The systematic instrumental error is believed to be negligible in this experiment. The statistical error in the counting process was normally less than 1% of the determination of the energy of a particular phonon. However, owing to the difficulty of assigning a proper background function to the peak-fitting routine and effect (iii) above, we found that different determinations of the same phonon energy sometimes disagreed by approximately 2%. Thus we have chosen to assign $\pm 2\%$ as our minimum error on all phonon measurements. In the case that the statistical error exceeds $\pm 2\%$, the quoted error has been set equal to the statistical error.

The phonon dispersion curves, as determined by the measured data, are presented in Fig. 1. The solid lines near $\vec{q} \rightarrow 0$, $\nu = 0$ represent the initial slopes of the acoustic modes as calculated from the elastic constants measured by McSkimin

*et al.*⁵ Error bars are shown only for those cases where the errors in Table I are larger than the size of the points in the figure. No measurements of the frequencies of the LO modes for $\vec{q} = 0$ are reported. Concerning the behavior of the LO mode near the zone center, it is to be noted that free-carrier screening effects⁶⁻⁸ become appreciable for $q \lesssim (6\pi n e^2 / \epsilon_F)^{1/2}$, where n is the carrier concentration and ϵ_F the carrier Fermi energy. For the carrier concentration in our GaSb crystal this wave vector has a magnitude of about $0.1(2\pi/a)$. The unperturbed plasma frequency of the free carriers is given by $\nu_p^e = [n e^2 / \pi m^* \epsilon(\infty)]^{1/2}$, which is about 3.4 THz.⁹ Thus one might expect plasmon-LO-phonon coupling effects in this energy region. A discussion of the neutron scattering from such modes has been given by Cochran *et al.*⁷

Unfortunately, the instrumental resolution in the experiment was sufficiently broad to preclude

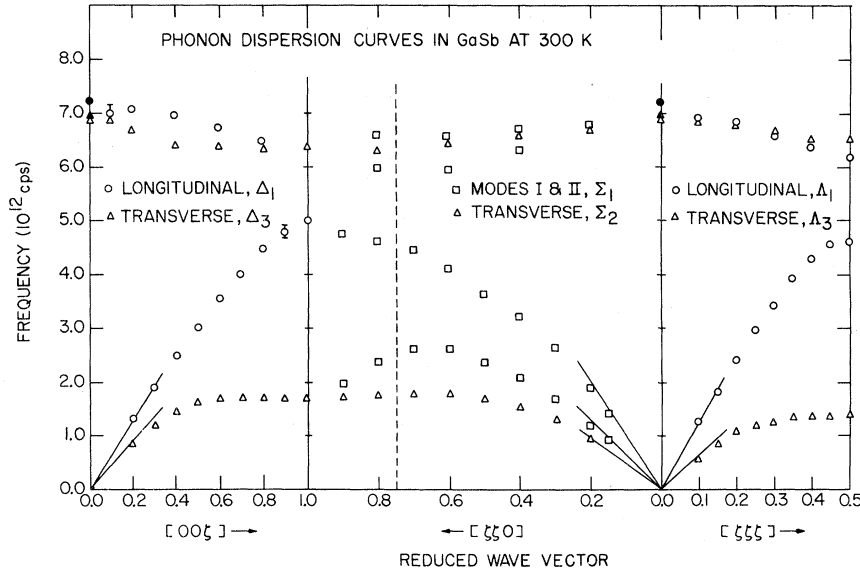


FIG. 1. Measured phonon dispersion curves in GaSb at 300 K. The solid lines near $\vec{q}=0, \nu=0$ represent the initial slopes of the acoustic modes as calculated from the elastic constants published in Ref. 5. The solid circles are the LO- and TO-mode frequencies taken from the infrared reflectivity measurements given in Ref. 10.

any detailed study of such effects for small \vec{q} . However, an apparent dip in the LO-mode frequency at $q = 0.1$ in the [001] and [111] directions was observed. This could be due to the carrier effects mentioned above, but it is also to be noted that the instrumental resolution was such that contamination of the LO-branch observations by the TO modes could not be completely eliminated. Such effects would also have a tendency to lower the measured LO-mode frequency. However, reducing our instrumental vertical collimation from $\pm 3^\circ$ to $\pm 1^\circ$, which should have reduced the TO-mode contamination effect, had no effect on the observed spectra at small \vec{q} .

Also shown in Fig. 1 are the values of the zone-center LO- and TO-mode frequencies obtained from infrared reflectivity measurements¹⁰ at 4 K, where free-carrier effects were apparently not observed. It may be seen that they represent a reasonable extrapolation (from large \vec{q}) of the neutron LO and TO dispersion curves.

III. SHELL MODEL AND ANALYSIS OF THE DATA

In order to obtain a convenient interpolation scheme for the phonon frequencies throughout the zone, we have analyzed the GaSb dispersion curves in terms of the shell model (SM). The formulation of the SM has been previously presented by several authors.¹¹⁻¹⁵ Following the usual procedure¹² in assuming the shell masses to be negligible with respect to the core masses, we can write the equations of motion for the displacement \underline{U} of the nuclei from their equilibrium positions as $\omega^2 \underline{M}\underline{U} = [\underline{R} + \underline{Z}\underline{C}\underline{Z} - (\underline{T} + \underline{Z}\underline{C}\underline{Y})(\underline{\xi} + \underline{Y}\underline{C}\underline{Y})^{-1}(\underline{T}^\dagger + \underline{Y}\underline{C}\underline{Z})]\underline{U}$, where the \underline{R} and \underline{T} matrices represent short-range interactions between ion and ion and ion and shell,

respectively; \underline{C} is the Coulombic interaction matrix, \underline{Y} the shell-charge matrix, \underline{Z} the ion-charge matrix, and $\underline{\xi}$ contains both self-energy terms and the \underline{S} matrix which describes the shell-shell short-range interactions. In the present calculations on GaSb, we utilized a form of the shell-model equations as adapted for the zinc-blende crystal structure by Dolling and Waugh¹ for use in their studies of GaAs. Dolling and Waugh's fourteen-parameter model (their model C) includes both first- and second-neighbor short-range interactions. This version was also used by Yarnell, Warren, Wenzel, and Dean² for their work on GaP and by Price, Rowe, and Nicklow³ for their analysis of the phonon spectrum of InSb. Excellent discussions of Dolling and Waugh's fourteen-parameter shell model can be found in Refs. 1, 3, and 16. Following Ref. 1, we have the following parameters: Z_1 , the charge on the Sb ion (the charge on the Ga ion is $-Z_1$); π_1, π_2 , the electronic (or atomic) polarizabilities of Sb and Ga, respectively; d_1, d_2 , the mechanical (or distortional) polarizabilities of Sb and Ga, respectively; $S_R = \alpha_S/\alpha_R$, the ratio of the diagonal shell-shell short-range force constant to the diagonal ion-ion short-range force constant for first neighbors; $\alpha_R (= \alpha_T)$, diagonal first-neighbor ion-ion force constant, $\gamma_R = \beta_R/\alpha_R$, $\gamma_T = \beta_T/\alpha_T$, and $\gamma_s = \beta_s/\alpha_s$, ratios of the first-neighbor short-range force constants for the ion-ion, ion-shell, and shell-shell interactions, respectively; μ, ν, λ , and δ second-neighbor short-range force constants.

As suggested by Cochran,¹² α_R is set equal to α_T to eliminate redundancy of the parameters without loss of generality. The number of parameters has been further reduced by assuming the following:

TABLE II. Values of shell-model parameters fitted to group III-V crystals.

	Set A	GaSb Set B	Set C	GaAs ^a	GaP ^b	InSb ^c	Units ^d
α_R	10.52 ± 0.179	10.66 ± 0.681	13.02 ± 0.155	19.67	32.68	12.08	e^2/Ω
Z_1	-0.136 ± 0.017	0.169 ± 0.028	0.037 ± 0.049	-0.018	0.31	-0.061	e
π_1	0.062 ± 0.004	0.100 ± 0.015	0.084 ± 0.019	0.075	0.018	0.085	none
π_2	0.097 ± 0.007	0.060 ± 0.032	0.022 ± 0.002	0.014	0.012	0.069	none
d_1	0.432 ± 0.023	0.674 ± 0.077	1.057 ± 0.034	1.588	1.277	0.677	none
d_2	0.653 ± 0.034	0.466 ± 0.092	0.187 ± 0.021	0.714	0.990	0.823	none
S_R	1.967 ± 0.556	1.813 ± 0.958	2.458 ± 0.116	1.267	1.173	1.491	none
γ_R	0.466 ± 0.018	0.367 ± 0.130	0.720 ± 0.004	0.222	0.335	0.577	none
γ_T	-0.413 ± 0.125	-0.425 ± 0.284	0.719 ± 0.033	0.043	0.215	0.226	none
γ_S	-2.431 ± 1.153	-2.285 ± 2.236	0.954 ± 0.015	-0.133	0.097	-1.163	none
μ	0.312 ± 0.022	0.292 ± 0.119		-0.815	-2.35	0.055	e^2/Ω
λ	0.471 ± 0.061	-0.717 ± 0.163		-1.941	-2.76	-0.470	e^2/Ω
ν	0.785 ± 0.058	0.923 ± 0.229		0.736	-0.51	0.499	e^2/Ω
δ	0.394 ± 0.040	0.302 ± 0.131		0.55	2.14	0.534	e^2/Ω

^aReference 1.^bReference 2.^cReference 3.^d Ω is the volume of the unit cell and e is the electron charge.

(a) The Sb-core-Ga-shell and Ga-core-Sb-shell short-range interactions are equal.

(b) The constants for the second-neighbor R , T , and S interactions are in the ratio of 1:1: S_R , or $\mu_R = \mu_T = \mu_s/S_R \equiv \mu$, etc., where $S_R = \alpha_s/\alpha_R$.

(c) The III-III and V-V interactions are identical or $\mu_R(1) = \mu_R(2) = \mu_R$, etc.

Explicit expressions for the elastic and dielectric properties of crystals with the zinc-blende structure have been given in terms of the above shell model by Cowley¹⁷ and Price *et al.*³ The expressions presented by the latter group have been used in the following.

The second-nearest-neighbor shell model was

used to fit the experimental data for GaSb. The data used in the fitting procedure included the three elastic constants,⁵ the high- and low-frequency dielectric constants,¹⁰ the piezoelectric constant,¹⁸ the squares of the LO and TO zone-center phonon frequencies determined from infrared data,¹⁰ and the 64 phonon frequencies measured in the present experiment (including data from each measured branch), for a total of 72 measured values. The squared phonon frequencies ν_i^2 were weighted in the fitting by the inverse of $2\nu_i\Delta\nu_i$. The other constants were weighted by the reciprocals of their respective uncertainties. In the final steps of the fitting procedure, the uncer-

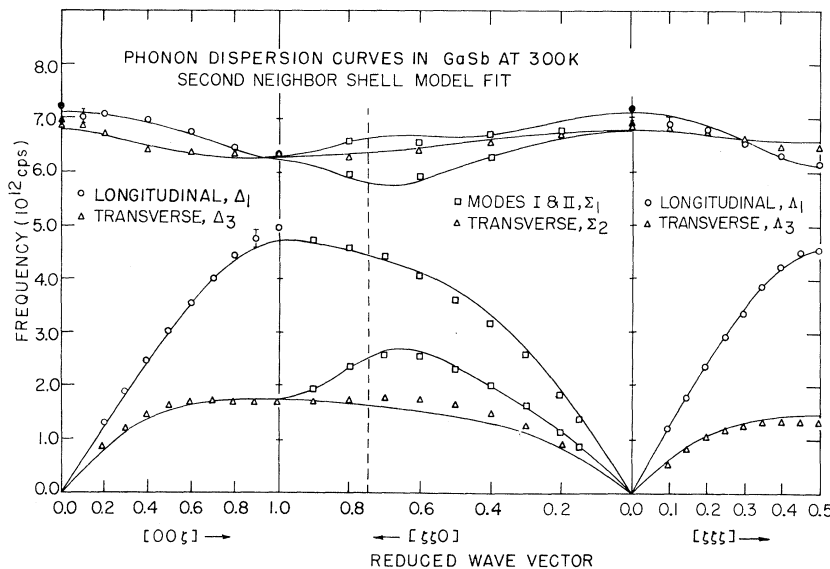


FIG. 2. Comparison of the measured phonon data points with the best-fit calculation of the second-neighbor shell model (referred to as set A in Tables II and III).

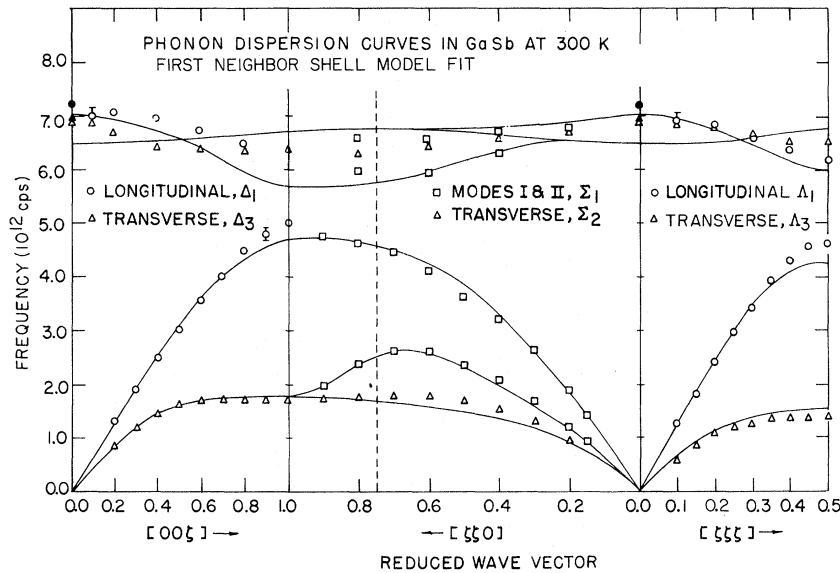


FIG. 3. Comparison of the measured phonon data points with the best-fit calculation of the first-neighbor shell model referred to as set C in (Tables II, III, and IV).

tainties for all these other constants were set equal to twice the published uncertainties to determine their influence on our fits to the neutron data. This increase in the errors caused little change in the fitted model parameters.

A computer program obtained from Price and Rowe of the Argonne National Laboratory was used to perform a nonlinear least-squares fit of the shell-model parameters to the GaSb data. We utilized the best-fit values of the parameters calculated for GaAs,¹ InSb,³ and GaP (Ref. 2) as our initial sets of parameters. However, since convergence was extremely slow and incomplete, we abandoned the fit started from the GaP parameters. We continued fitting the other two sets of parameters until improvement in the fits, using the standard χ^2 criteria, was no longer significant. The final values χ^2 for these two sets of parameters were almost equal, although the parameter values were different in most cases. The inability to find a unique set of parameters has been encountered in each of the previous applications of the fourteen parameter shell model to the III-V semiconductors. Thus it was not surprising that we also were unable to find a unique parameter set. We decided not to carry out the complete fitting procedure for other sets of initial parameters since the procedure is costly and the existence of several minima in the fourteen dimensional parameter space indicated that the likelihood of finding a unique minimum was very small.

We carried to completion three different approaches to the fitting procedure:

(i) We started with the published parameters for InSb. Our resulting fit is given as parameter set A.

(ii) We started with the published parameters for GaAs; our resulting fit is given as set B.

(iii) We attempted fits allowing only *first-neighbor* short-range and long-range Coulomb interactions by fixing the four second-neighbor parameters μ , λ , ν , and δ equal to zero. We started with our sets A and B, and the fits converged to results not significantly different from one another. We present the best-fit results as set C. The final parameters (and their errors determined by the standard covariance matrix technique) for these three approaches are presented in Table II along with the published second-nearest-neighbor shell-model-fit values for GaAs, GaP, and InSb. The χ^2 values are set A, 3.53, set B, 3.62, and set C, 5.86. However, the parameters in each set are poorly determined and highly correlated.

The theoretical dispersion curves calculated using set A are shown in Fig. 2. The curves calculated using set B are not significantly different from the set-A curves. The curves calculated

TABLE III. Comparison of the elastic and dielectric properties of GaSb.

Property	Observed	Calculated			Units
		Set A	Set B	Set C	
C_{11}	8.839 ± 0.008^a	8.70	8.69	8.70	10^{11} dyn/cm ³
C_{12}	4.033 ± 0.010^a	4.11	4.13	3.82	10^{11} dyn/cm ³
C_{44}	4.316 ± 0.004^a	4.19	4.20	4.18	10^{11} dyn/cm ³
ϵ_0	15.69 ^b	13.99	14.69	16.70	none
ϵ_∞	14.44 ^b	12.79	13.32	14.45	none
e_{14}	-3.78 ± 0.76^c	-3.63	-3.86	-3.85	10^4 esu/cm ²
ν_{TO}	6.87 ± 0.03^d	6.80	6.77	6.55	10^{12} cps
	6.915 ± 0.09^b				10^{12} cps
ν_{LO}	7.209 ± 0.06^b	7.12	7.11	7.04	10^{12} cps

^aReference 5.

^bReference 10.

^cReference 18.

^dThis work.

TABLE IV. Values of parameters from first-neighbor shell-model fits to published phonon dispersion curves of III-V gallium compounds.

	GaSb ^a	GaAs ^b	GaP ^c	Units ^d
α_R	13.02 ± 0.155	13.63	14.66	e^2/Ω
Z_1	0.037 ± 0.049	0.123	0.398	e
π_1	0.084 ± 0.019	0.076	0.025	none
π_2	0.022 ± 0.002	0.010	0.018	none
d_1	1.057 ± 0.034	1.160	0.827	none
d_2	0.187 ± 0.021	0.447	0.644	none
S_R	2.458 ± 0.116	1.734	1.560	none
γ_R	0.720 ± 0.004	0.543	0.668	none
γ_T	0.719 ± 0.033	0.262	0.421	none
γ_S	0.954 ± 0.015	0.187	0.273	none

^aErrors determined by standard covariance matrix technique.

^bOur fit to data in Ref. 1.

^cOur fit to data in Ref. 2.

^d Ω is the volume of the unit cell and e is the electronic charge.

from set C are shown in Fig. 3. The non-neutron data used in the fitting, together with their fitted values, are shown in Table III. The set-A shell-model (SM) curves agree with the measured dispersion curves within about 5%, except in the Σ_2 (A) branch, where the deviation is as great as 15%. The observed discrepancy in the Σ_2 (A) branch was also evident in the SM fits reported for¹ GaAs and² GaP. The Σ_2 (A) branch in³ InSb was not measured. However, in the cases of both GaAs and GaP no data from the [110] direction were used in the SM fitting procedure. We had expected that the inclusion of data from the [110] modes would provide a better fit to the Σ_2 (A) branch. It appears that the SM is unable to fit the Σ_2 (A) branch of these compounds satisfactorily.

The first-neighbor SM curves (from set C) provide a somewhat poorer fit to the measured data, although even these curves are quite reasonable.

We were unable to find any sound basis for choosing either SM parameter sets A or B as being more physically realistic. The dispersion curves calculated from both sets are almost identical, and a comparison of inelastic structure factors calculated with each set reveals no major difference in predicted phonon intensities. However, it is interesting to compare the SM parameters for the three gallium compounds GaP, GaAs, and GaSb, since several systematic trends among the SM parameters for the gallium compounds can be seen. In order to make a meaningful comparison for the three compounds, we decided to compare first-neighbor shell models only. It is likely that with second-neighbor shell models the physical significance of the parameters is decreased, although the fit may be improved. In order to obtain the best first-neighbor shell-model fits to GaAs and GaP we fitted the published phonon dispersion curves^{1,2} in all three principal symmetry directions for these two materials. We used as initial values of the parameters those given in the published second-neighbor shell-model fits. The parameters obtained from our first-neighbor shell-model fits (along with set C for GaSb) are shown in Table IV.

In going from GaP through GaAs to GaSb it may be seen that (a) the nearest-neighbor III-V ion-ion force constant α_R , is of same order; (b) the electronic polarizability of the group-V ion π_1 increases; (c) the magnitude of the ionic charge decreases; (d) The mechanical polarizability of the Ga ion d_2 decreases; and (e) the ratio S_R of the III-V shell-shell force constant to the III-V ion-ion force constant becomes larger. Furthermore, since

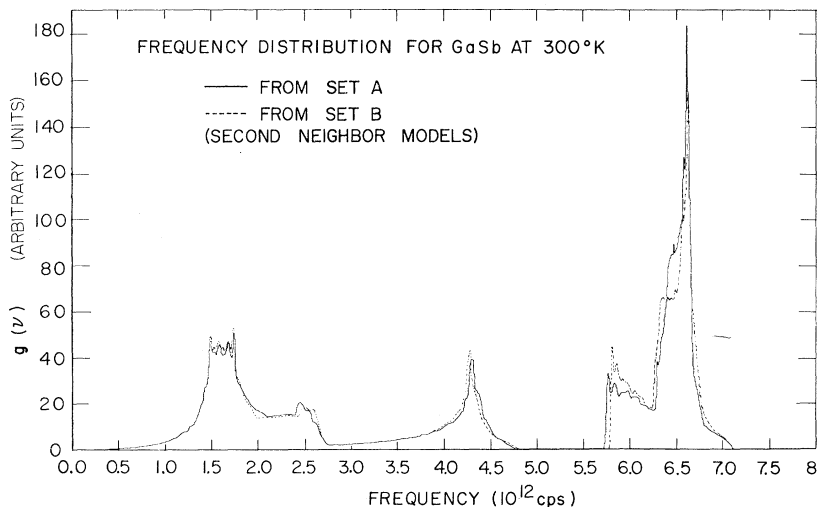


FIG. 4. Phono frequency distribution for GaSb as calculated from the second-neighbor shell models. The two lines correspond to the two sets of parameters, sets A and B, as given in Table II. It is not possible to ascribe physical significance to the minor differences between the two calculations.

$S_R = \alpha_s / \alpha_R$, calculations show that α_s increases.

It is also interesting to compare trends in the reduced TO-mode frequency ν_{TO} / ν_p^i , where ν_p^i is the ionic plasma frequency for the material in question. Note that ν_{TO} is not directly affected by the macroscopic field and hence depends only on the "intrinsic" force constants in the solid. We find the following values for ν_{TO} / ν_p^i : GaP, 1.536; GaAs, 1.540; GaSb, 1.65. We note that ν_{TO} / ν_p^i increases with ϵ_∞ and hence with the polarizability of the material. Such trends will be discussed from the viewpoint of a microscopic theory in a later publication.

Although the SM parameters are difficult to interpret physically, they are useful in calculating the phonon frequency distribution $g(\nu)$. We computed $g(\nu)$ for SM parameters sets A and B using the method of Gilat and Raubenheimer.¹⁹ The calculations were carried out using a computer program written by Price and Rowe. We used a frequency interval of 0.01×10^{12} cps in the calculations.

A plot of $g(\nu)$ for sets A and B is shown in Fig. 4. There are some discernible differences between the two $g(\nu)$'s shown. However, they exhibit similar major features, and it is not possible to ascribe significance to their discrepancies.

The above frequency distributions were used to calculate the lattice contribution to the heat capacity C_v and the Debye Θ for GaSb. There are no significant differences between the values calculated using set A and those determined using set B. The calculated values for C_v and Θ_D along with the experimental data from Piesbergen,²⁰ Cetas, Tilford, and Swenson,²¹ and Holste,²² are shown in Figs. 5 and 6. The discrepancies between the measured and calculated values for Debye Θ at

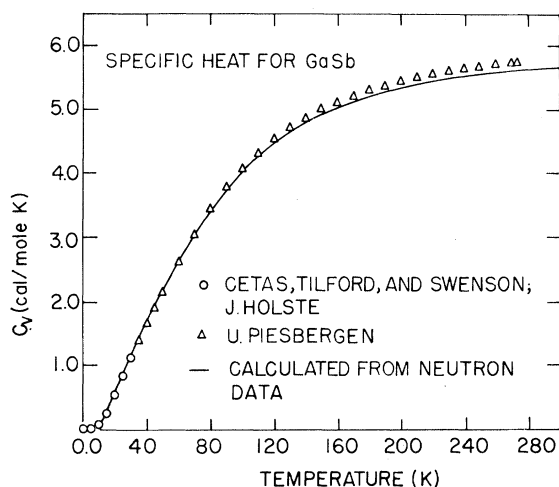


FIG. 5. Comparison of heat capacity of GaSb calculated from our $g(\nu)$ with the measurements given in Refs. 20–22.

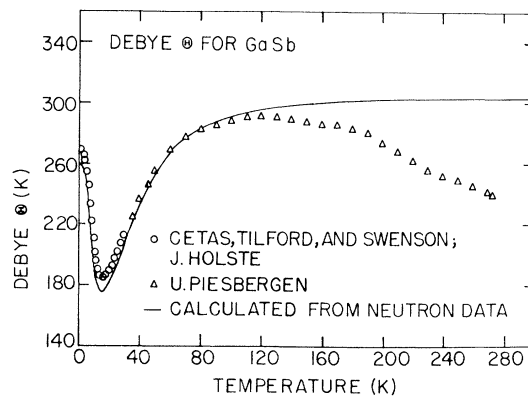


FIG. 6. Comparison of the Debye temperature for GaSb calculated from our $g(\nu)$ with the measurements given in Refs. 20–22. The large discrepancies at high temperature are discussed in the text.

high temperatures are not believed to be as significant as the large deviation suggests. The data in Ref. 20 are not presented with uncertainties; because of the difficulty of measuring small changes in C_v at high temperature, we believe that the possible uncertainties in the measured values for Debye Θ could be quite large.

SUMMARY AND DISCUSSION

We have presented the results of inelastic neutron scattering measurements of the phonon dispersion curves along the principal symmetry directions of GaSb at 300 K. The shell model has been used to analyze the data primarily in order to obtain a reasonable interpolation scheme for calculating the complete phonon spectrum and the frequency distribution function. Specific-heat calculations based on the latter are in reasonable agreement with experiment. The nonuniqueness and apparent lack of physical significance of the shell-model parameters indicate, as in the case of the other III-V compounds, the need for a more microscopically based calculation of the phonon spectra in these compounds. Possible approaches are the microscopically based generalized screening model²³ or the band-charge model.²⁴ The heteropolar nature of these compounds renders a microscopic calculation considerably more complicated than those already performed for the homopolar group-IV elements.²³ Such approaches are currently under investigation.

ACKNOWLEDGMENTS

We wish to thank Texas Instruments, Ltd. for supplying the GaSb crystal used in the experiments, Howard Shanks for kindly supplying the information for carrier concentrations in the sample, and G.

C. Danielson for useful discussions. We also wish to thank D. L. Price and J. M. Rowe for

making available listings of their shell-model fitting programs and for helpful discussions.

*Present address: Feltman Research Laboratory, Picatinny Arsenal, Dover, N. J. 07801.

¹G. Dolling and J. L. T. Waugh, in *Lattice Dynamics*, edited by R. F. Wallis (Pergamon, Oxford, 1965), p. 19.

²J. L. Yarnell, J. L. Warren, and R. G. Wenzel, in *Neutron Inelastic Scattering* (IAEA, Vienna, 1968), Vol. 1, p. 301.

³D. L. Price, J. M. Rowe, and R. M. Nicklow, *Phys. Rev. B* **3**, 1268 (1971).

⁴M. E. Straumanis and C. D. Kim, *J. Appl. Phys.* **36**, 3822 (1965).

⁵H. J. McSkimin, A. Jayaraman, P. Andreatch, Jr., and T. B. Bateman, *J. Appl. Phys.* **39**, 4127 (1968).

⁶B. B. Varga, *Phys. Rev.* **137**, A1896 (1965); K. S. Singwi and M. P. Tosi, *ibid.* **147**, 658 (1966).

⁷W. Cochran, R. A. Cowley, G. Dolling, and M. M. Elcombe, *Proc. R. Soc. A* **293**, 433 (1966).

⁸M. A. Omar, *Phys. Rev.* **186**, 791 (1969).

⁹The value of the effective hole mass m_h^* used in this calculation was obtained from C. Hilsun, in *Proceedings of Seventh International Conference on the Physics of Semiconductors*, edited by M. Hulin (Dunod, Paris, 1964), p. 1131.

¹⁰M. Hass and B. W. Henvis, *J. Phys. Chem. Solids* **23**,

1099 (1962).

¹¹V. S. Mashkevitch and K. B. Tolpygo, *Zh. Eksp. Teor. Fiz.* **32**, 520 (1957) [*Sov. Phys.-JETP* **5**, 435 (1957)].

¹²W. Cochran, *Proc. R. Soc. A* **253**, 260 (1959).

¹³B. G. Dick and A. W. Ovenhauser, *Phys. Rev.* **112**, 90 (1958).

¹⁴A. D. B. Woods, W. Cochran, and B. N. Brockhouse, *Phys. Rev.* **119**, 980 (1960).

¹⁵R. A. Cowley, W. Cochran, B. N. Brockhouse, and A. D. B. Woods, *Phys. Rev.* **131**, 1030 (1963).

¹⁶S. K. Sinha, *Crit. Rev. Solid State Sci.* **3**, 273, 1973.

¹⁷R. A. Cowley, *Proc. R. Soc. A* **268**, 121 (1962).

¹⁸H. J. Hrostowski and C. S. Fuller, *J. Phys. Chem. Solids* **4**, 155 (1958).

¹⁹G. Gilat and L. J. Raubenheimer, *Phys. Rev.* **144**, 390 (1966).

²⁰U. Piesbergen, *Z. Naturforsch. A* **18**, 141 (1963).

²¹T. C. Cetas, C. R. Tilford, and C. A. Swenson, *Phys. Rev.* **174**, 835 (1968).

²²J. C. Holste, *Phys. Rev. B* **6**, 2495 (1972).

²³S. K. Sinha, R. P. Gupta, and D. L. Price, *Phys. Rev. Lett.* **26**, 1324 (1971); *Phys. Rev. B* **9**, 2564 (1974); **9**, 2573 (1974).

²⁴R. M. Martin, *Phys. Rev.* **186**, 871 (1969).